2022

Object Tracking-based Droplet Characterization on High Flowrate Electrospray for PM Removal

Minkyu Jung

Soyeon Kim

Donik Ku

Sanghun Jeong

Soojin Bae

See next page for additional authors

Object Tracking-based Droplet Characterization on High Flowrate Electrospray for PM Removal

Minkyu Jung[1], Soyeon Kim[2], Donik Ku[3], Sanghun Jeong[4], Soojin Bae[5], Gijeong Seo[6], Minsung Kim*

[1,2,3,4,5,*]Department of Intelligent Energy and Industry, Chung-Ang University, 06975, Seoul, Republic of Korea
([1]mamba24@cau.ac.kr, [2]nuri36@cau.ac.kr, [3]ehsdlr@cau.ac.kr, [4]suj531@cau.ac.kr, [5]sooj980809@cau.ac.kr)

[6,*]School of Energy Systems Engineering, Chung-Ang University, 06975, Seoul, Republic of Korea
([6]koki8235@cau.ac.kr)

* Corresponding Author (+82-2-820-5973, *minsungk@cau.ac.kr)

ABSTRACT

Electrospray is a phenomenon of liquid atomized into small droplets when subjected to high electrostatic potential difference. The cone-jet mode, which forms a stable cone and produces fine monodisperse droplets has been mostly focused on the previous studies. Flowrate of the cone-jet mode were limited at only few microliter/min scale to prevent corona discharge. However, in the electrospray mode for particulate matter removal, high flowrate of several milliliter/min is used to obtain a sufficient liquid-to-gas ratio. In this high flowrate condition, the applied voltage required to atomize the liquid increases, and 2D and 3D spraying mode that have not been shown in previous studies appears. In this study, the electrospray droplet diameter under high flowrate condition was measured by the shadowgraph method using a high-speed camera. Multi-layer image processing algorithm was employed in order to measure the droplet diameter from pixel occupied in the original image. Bias caused by the difference in the probability of being included in the image depending on the speed of the droplet, was corrected through object tracking. Finally, corrected droplet diameter distribution of each spraying mode under high flowrate condition was measured. Results of this study provide new guidance for calculating the droplet lifetime surviving evaporation and dust collection efficiency in an actual scrubber condition.

1. INTRODUCTION

As the social interest on particulate matter has been increased nowadays, environmental standards and regulations at emission of air pollutants are being strengthened all around the world. Power plants, emits large amount of air pollutants, use wet scrubbers as exhaust gas treatment systems. In order to overcome its large water consumption, electrospray was adopted. Electrospray is a phenomenon that the working fluid sprayed into small droplets when passing through the nozzle tip with high electrostatic charge induced. Fig. 1 shows the mechanism of PM removal with electrospray. After dispersion, charged droplets collide with positively charged PM, and removed by cleansing water at the collecting electrode. Flowrate of the working fluid and the applied voltage have the greatest influence on determining the electrospray mode. In previous electrospray research, ‘Cone-jet mode’, which is the most characteristic mode among the various modes has been focused (Borra, 2018). Stable cone and the jet are formulated at the end of the nozzle when the electric shear stress, surface tension and the hydraulic pressure are at the equilibrium (Jaworek and Krupa, 1999). Taylor (1966) named the stable cone as “Taylor cone” and calculated the theoretical half-angle of the cone to be 49.3°. Then the liquid elongated into thin jet by electrostatic repulsive force and atomized into fine droplets.

Cone-jet mode has been applied in various fields such as coating and EHD printing because the stability of the spray is very high, and the produced droplets are fine and uniform (Tang and Gomez, 1994). The flowrate conditions of

the cone-jet mode studies were limited under few microliters per minute (Cloupeau, 1994). This is because, as the flow rate increases, the applied voltage required for atomization also increases and causes corona discharge that prevents stable cone formation (Kim *et al.*, 2011, Park et al., 2014). However, the flowrate of the electroscurbber has to be up to several milliliter per minute in order to increase the contact area with the flue gas for better collection efficiency. Moreover, required applied voltage also increased up to several tens of kV and having a different spray mode from the previous electrospray studies. Cho *et al.* (2019) classified the spray modes of high flowrate electrospray for PM removal, and Kim *et al.* (2019) visualized each mode and studied about the discharge characteristics with respect to electric conductivity of working fluids.

In the case of high flowrate spraying mode (2D 3D spraying mode) for PM collection, range of the spray is wider, and the spray density is lower than the cone-jet mode. Therefore, conventional method for measuring the size of the electrospray droplets, for example PDA method, cannot be used. This is because PDA measures the size of a particle that passing the measuring point, so in the case of sparse spray like 3D spray, the representativeness of the distribution is very low. Also, as a result of the measurement, the distribution was not well measured, so that the study on the measurement of the spray droplet size of high-flowrate electrostatic spraying for dust collection through the imaging method was conducted (Jung *et al*., 2022).

With the development of cameras, the accuracy of the imaging method of measuring the size through the pixels occupied by the object captured in the picture has increased. And the several research has been conducted to measure the size distribution of particles through the imaging method in various particle generations. However, when the droplet size distribution is measured using the imaging method, an error in the distribution according to the particle velocity occurs. In the case of droplets with different velocities, there is a difference in the probability of being included in the image, and a biased distribution is obtained. In the present study, various spraying modes at high flowrate conditions were visualized through a high-speed camera, and the size of the spray droplets were measured through multi-stage image processing. After image processing at one frame, same process has been applied sequentially to the next frame image. Object track has been constructed through every frame with detected droplet data. Biased droplet diameter distribution and the corrected distribution were measured and compared. As a result, smaller-lighter droplets were underestimated, and the larger-heavier droplets were overcounted to the distribution. When measured without an object tracking method, a bimodal distribution appears unlike the actual spray distribution, and the actual spray distribution follows a lognormal distribution. In addition, the velocity distribution of the electrospray droplets was measured through the analysis of each frame of the high-speed camera.

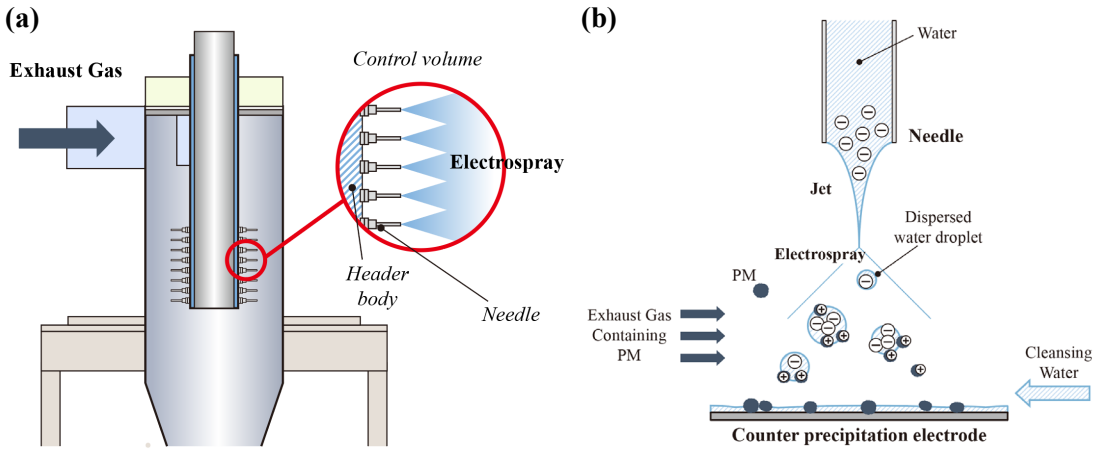

Figure 1: (a) Diagram inside the electroscrubber, (b) Mechanism of electrospray precipitation

2. EXPERIMENTAL SETUP

Fig. 2(a) shows the experimental setup of present study. Flowrate of the working fluid and applied voltage were set with a syringe pump and a high-voltage DC power supply. The high-voltage power supply is attached to a stainless-steel nozzle so that the working fluid passing through the nozzle is charged into negative voltage. To prevent the electricity leakage, the nozzle and the ground plate is located in acrylic chamber because the voltage condition of this study is high enough to exceed the electrical breakdown voltage of air. Experimental conditions and properties

of the working fluid were summarized at Table 1. As mentioned above, flowrate of this study was 10 and 15 mL/min, which is tens of times larger than typical nanoscale electrospray studies. Applied voltage was adjusted in –5 kV increments from 0 kV to –30 kV, until the arc discharge initiate.

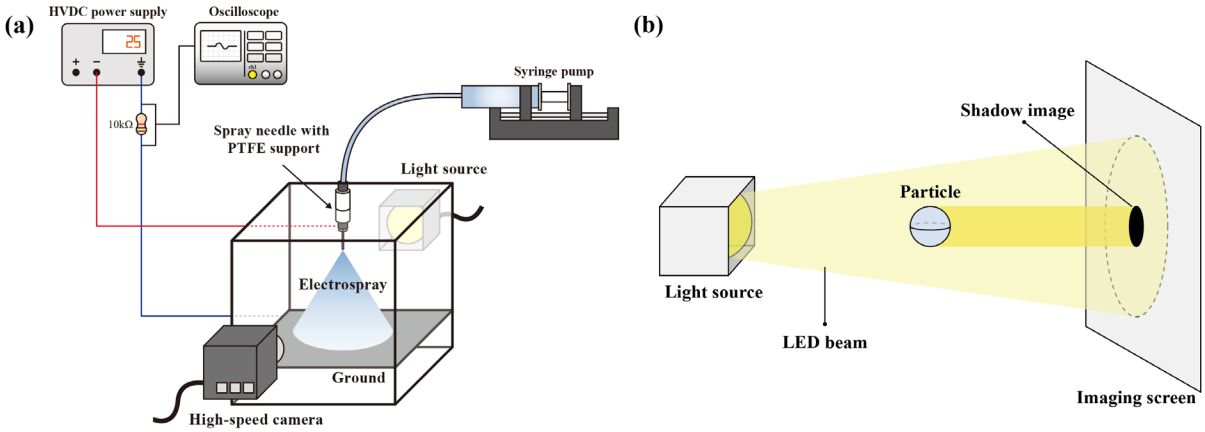

Figure 2: (a) Schematic diagram of experimental setup, (b) Working principle of shadowgraph

Table 1: Experimental conditions and parameter setup

Parameter	**Specification**	**Range**	**Unit**	**Remarks**
Electrospray	Applied voltage (V)	0 ~ 30	-kV	Negative DC
	Flow rate (Q)	5 ~ 15	mL/min	
	Nozzle to plate distance (h)	50	mm	
Nozzle	Gauge	18/21	G	Stainless steel
	Inner diameter (d_0)	0.86/0.5	mm	
	Outer diameter	1.26/0.8	mm	
Working fluid	Density (ρ)	997	kg/m^3	Distilled water
	Electric conductivity (K)	1.20×10^{-4}	S/m	
	Surface tension (γ)	0.072	N/m	
	Permittivity of vacuum (ε_0)	8.854×10^{-12}	F/m	
	Dielectric constant (ε)	80.2	-	
High-speed camera	Frame rate	4000	fps	

Trajectories of the moving droplets were visualized with high-speed camera due to the high velocity of electrospray droplets. High shutter speed not only makes object tracking easier, but also enables to measure the droplet velocity. Shadowgraph is a non-intrusive method for particle size measurement that is independent of particle shape and spray structure. A light source, particles, and the imaging device must be aligned on the same line as shown in Fig. 2(b) to obtain a shadowgraph image. A light that does not pass through the particles is reflected or refracted, creating a shadow of the particles in the image.

In high flowrate electrospray in this study, the spray range of droplets sprayed from a single nozzle is very wide, about a circle with a diameter of 30 cm. Therefore, in order to capture all the droplets in this range, the distance between the camera and the nozzle must be relatively long. At this time, in order to be able to shoot all the small droplets, the maximum shutter speed that does not reduce the image size was set to 4000. In addition, a 100mm macro lens was used for the lens used for image shooting. Moreover, in order not to blur the droplets in front and back as much as possible based on the nozzle, the aperture was tightened to secure a wide field of view.

Fig. 3 shows typical images of high flowrate electrospray with the optical configuration explained before. In Fig. 3, distilled water was supplied to the nozzle with a flowrate of 5mL/min, and the applied voltage was set as -12.8kV. Each image in Fig. 3 is an image extracted from a larger set of experiments, at the time intervals of 2.5μs to make it easy to check the movement of spray droplets.

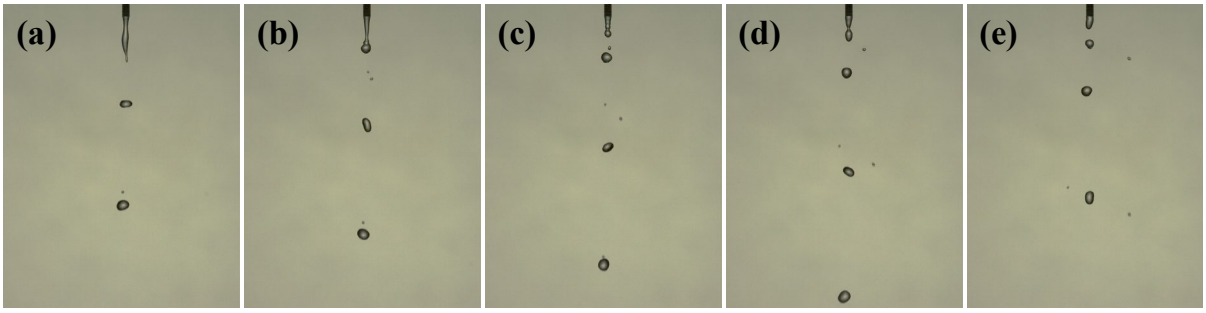

Figure 3: Examples of high-speed camera images of electrospray droplets

3. EXPERIMENTAL RESULTS

3.1 Image Processing

Sequence of image processing of high-speed camera image was shown in Figure 4. Entire image processing sequence were done with python languages and OpenCV libraries. Figure 4(a)~(f) show the original image, grayscale image, threshold image, noise removed image, edge detection image and the final labeled image, respectively.

Image processing has the greatest dominance in object tracking performance beyond entire process. At first, original RGB images were normalized in order to obtain homogenous background illumination. Normalized image was converted into 256-bit grayscale image and then binarized into B&W image with adaptive gaussian thresholding. Small salt and pepper noises included into binary image during the thresholding, were removed with median filter. Then droplets were subtracted from the background through the Suzuki's contour finding algorithm.

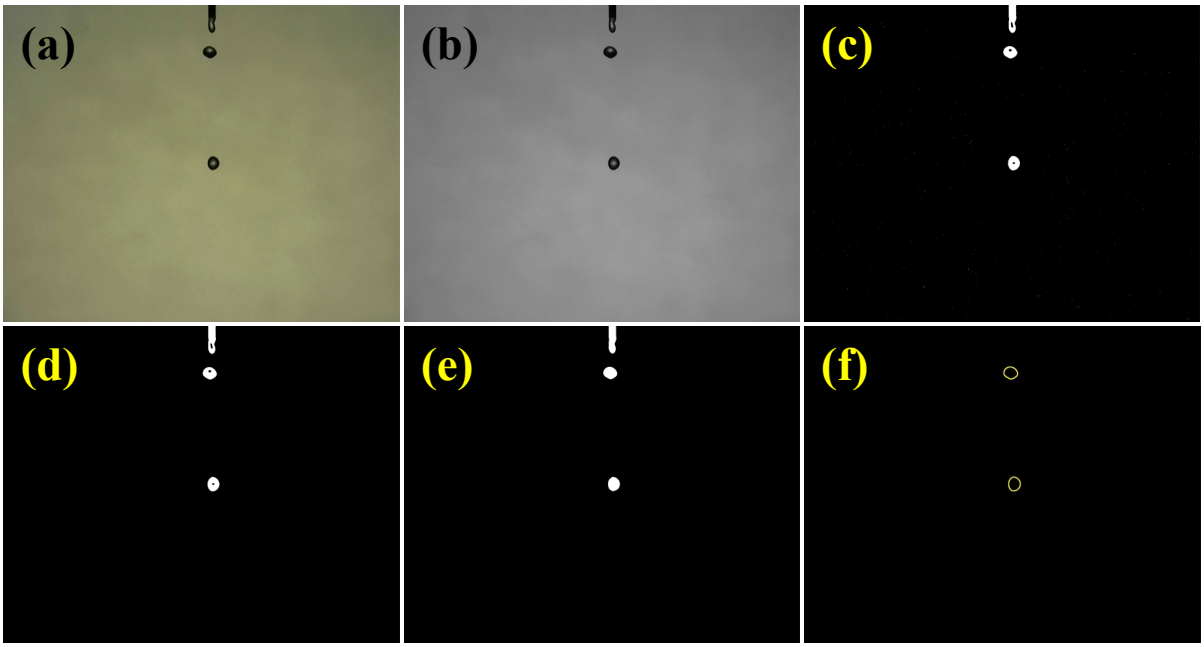

Figure 4: Sequences of image processing: (a) Original image, (b) Grayscale image, (c) Threshold image, (d) Noise removed image, (e) Edge detection image, (f) Final image

Unnecessary elements such as nozzle and the jet were filtered through the circularity. After detecting the droplets and the edges, the droplet diameter was measured by calculating the area of the separated droplet parts based on the outer diameter of the nozzle.

3.2 Object Tracking

As illustrated on the introduction, bias at the distribution due to the difference in velocities occurs. Taking a large and slow droplet as an example, in case of using high-speed camera that takes several shots in a short time, the droplet will be accumulated several times and results in overcounted in the size distribution. In addition, even if a normal DSLR shadowgraph is used or selecting the image randomly, there still is a difference in the probability that the droplet will be included in the region of interest within the instant the photo is taken, so this bias is unavoidable when using the imaging method. There are two possible solutions; first is to correct the bias with correlations between the size and velocity, and the second is to eliminate the bias by selecting the representative value among the track elements.

Object tracking from the recorded videos are comprises three stages. The image processing process described earlier is this stage. Second is to identify the detected objects of the next frame and then associate the same object. In this study, we designed an algorithm that can track the droplet through the physical characteristics of the droplet captured in each frame. In the first step, the size and centroid coordinates of the droplet were calculated through the image processing process, and the droplet with the smallest change in the size, moving distance, and moving angle of the droplet captured in each frame was judged as the same droplet. The last is to connect to the last frame of the video to form a track for each droplet.

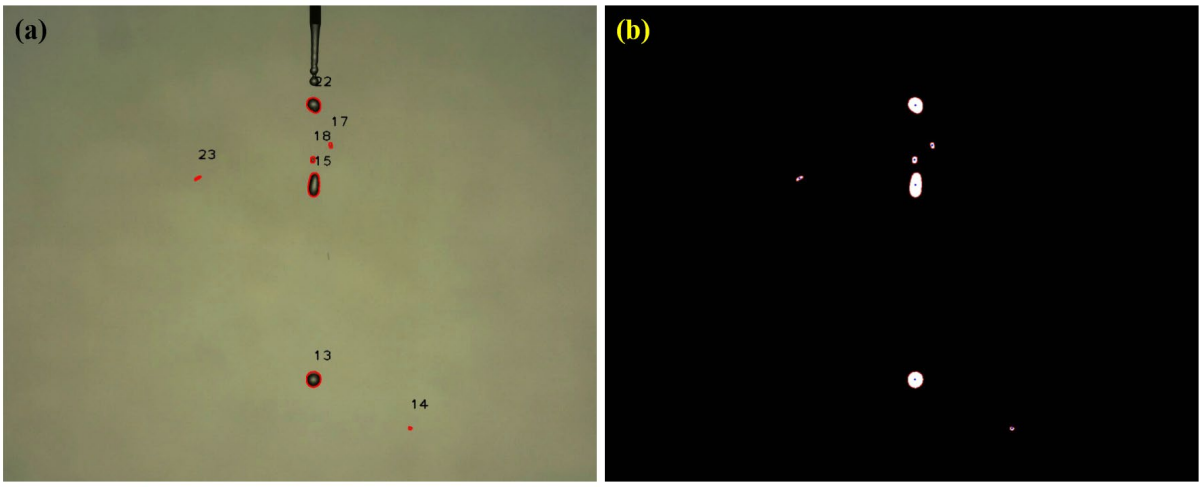

Figure 5: (a) Object tracking result, (b) Detected droplets at image processing during object tracking

Fig. 5 shows the snapshot of the tracking results of high flowrate electrospray image. 2180 frames of high-speed camera images were analyzed, and 10437 droplet data were obtained before tracking. As a result of object tracking, those 10437 raw data were identified as 417 droplets.

3.3 Droplet Characterization

Through image processing, droplet diameter distribution of distilled water electrospray (5 mL/min, -12.8 kV) was measured. The droplet size distribution obtained by analyzing the high-speed camera image in the usual way, that is, the bias distribution and the new droplet size distribution obtained using the object tracking method, that is to say the corrected distribution, were measured. Fig. 6 shows the comparison of biased distribution and the corrected distribution. According to the difference in the amount of data of the two distributions, both distributions were normalized and displayed as a histogram.

Biased distribution showed a bimodal distribution near 500μm and 1800μm. In addition, the peak probability density of small and large droplets was found to be similar. However, in the actual spray image, there are relatively more small droplets than large ones, indicating that there is an error in the distribution. On the other hand, in the case of the corrected distribution, it can be seen that small droplets of 500μm are predominantly generated compared to the large droplets. Droplets of 1000μm rarely exist, and droplets larger than 1500μm appears frequently. This is because large droplets are slow and thus overcounted in a biased distribution as they are captured much more in the high-speed camera image and are more included in the raw data. On the other hand, small droplets were underestimated at the biased distribution compared to the corrected distribution. Because small droplets are light in weight, so they are accelerated more due to the electrostatic field and highly charged liquid jet. According to the high-speed camera

image, it was confirmed that small droplets disappear rapidly from the center of the nozzle to the outside. As following, if the distribution error caused by the speed difference is not corrected, a large bias in the droplet distribution occurs.

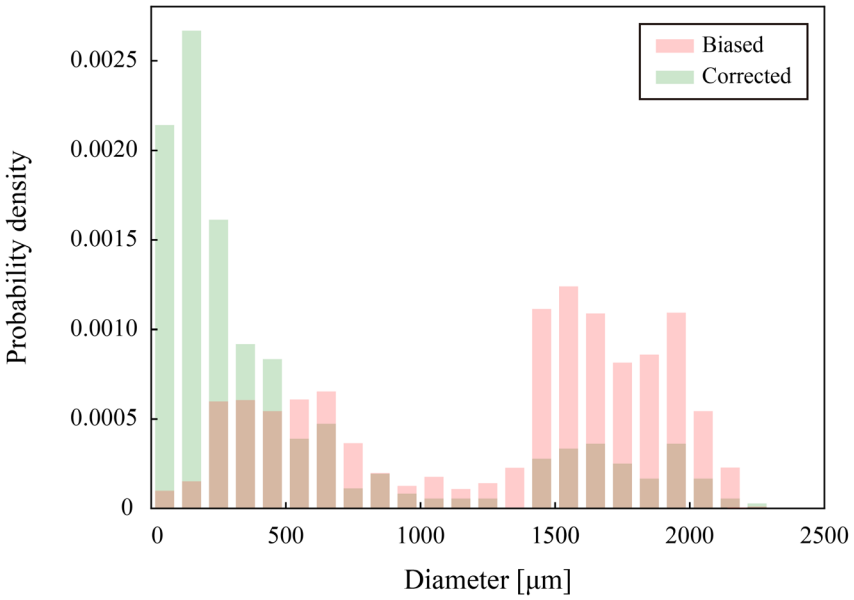

Figure 6: Comparison of biased and corrected droplet distribution

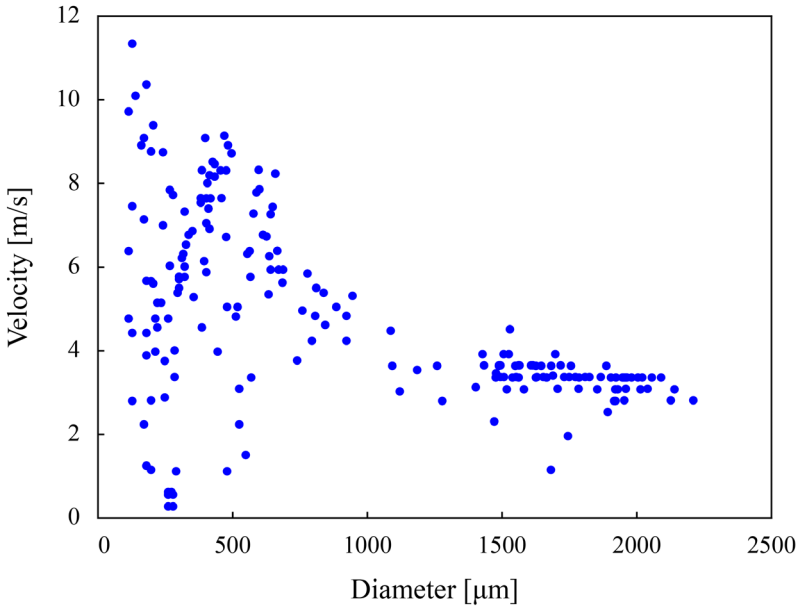

Figure 7: Droplet velocity verses droplet diameter

The velocity of each droplet was measured based on the centroid of droplets of the frames obtained through the object tracking. The average size and average velocity of the traced droplet from the start to the end of the track are shown in Fig. 7. Since the depth of field (DOF) in the image is negligible, the velocity of the droplet is calculated based on 2D trajectory. As shown in Fig. 7, the maximum velocity of the droplet tends to be inversely proportional to the size of the droplet. This explains why the distribution error appears. However, in the case of droplets smaller

than 500μm, droplets with low average velocity were observed. This is a special case of electrospray, and it occurs because the droplets are negatively charged after spraying. Fig. 8 is a diagram showing an example of the behavior of droplets during the distilled water electrospray, and the velocity distribution of droplets A and B after atomization. As shown in Fig. 8(a), droplet B is accelerated downward at a very high speed immediately after being atomized. However, after the frame 21, the velocity decreases and disappears due to the electrostatic repulsive force with the charged droplet A as it approaches the large droplet A that exists below vertically.

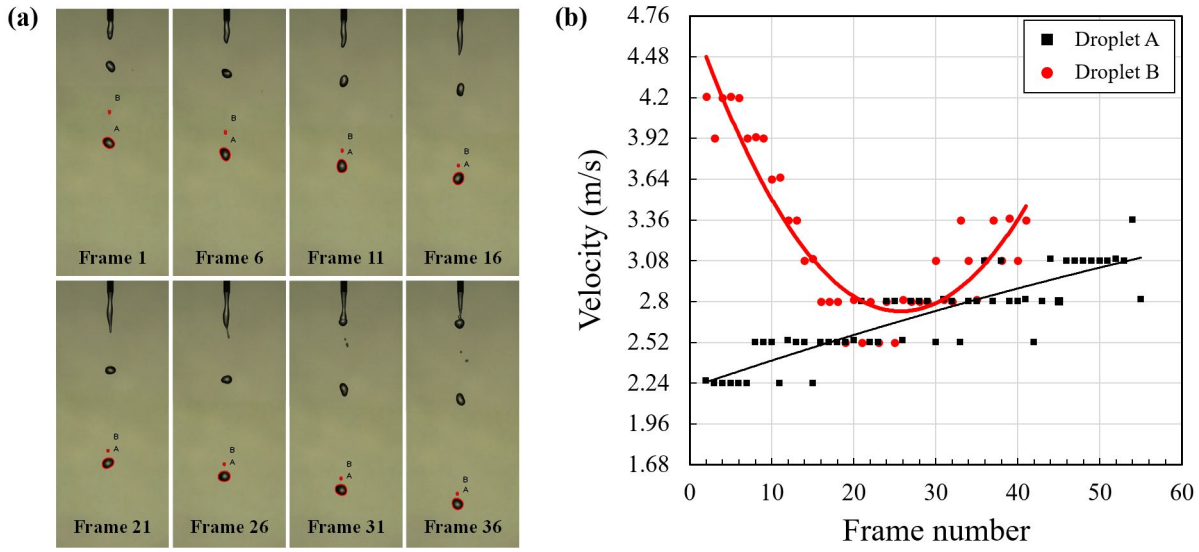

Figure 8: (a) Behavior of the electrostatic spray droplets, (b) Velocity changes of two droplets

For this reason, in the case of electrostatic spray droplets, it is difficult to clearly define the relationship between the droplets and the velocity. Therefore, when using the imaging method, the object tracking method should be used to correct the error caused by the speed difference.

4. CONCLUSIONS

In this study, a visualization-based study was conducted to measure the characteristics of droplets generated from the mode of high flowrate electrospray that can be applied to the electroscrubber precipitation system. Diameter of the spray droplet was measured by calculating based on the black pixel that spray droplet occupied in the high-speed camera image. High-speed camera images were preprocessed through multi-stage image processing algorithms. Additionally, biased of droplet diameter distribution due to the velocity difference were recognized and corrected with object tracking method.

Small, light droplets are rapidly accelerated by the electromagnetic field and disappear from the image plane, underestimated in the distribution measured in the usual way. On the other hand, since large droplets are overcounted for the same reason, the overall distribution is flattened, resulting in a bias. In case of electrospray, not only the jet, but also the sprayed droplets are charged, so the size and velocity relationship are not easily defined. In conclusion, a tracking method should be used for bias correction at droplet characterization with imaging method. As a follow-up study, electrostatic spray research on temperature and humidity in consideration of the above flue gas atmosphere characteristics is in progress.

NOMENCLATURE

V	applied voltage(negative)	(-kV)
Q	flow rate	(mL/min)
K	electric conductivity	(S/m)
h	distance of nozzle to plate	(mm)
d_0	nozzle inner diameter	(mm)

d_d	droplet diameter	(μm)
v_d	droplet velocity	(m/s)

Greek symbol

ρ	density	(kg/m^3)
γ	surface tension	(N/m)
ε_0	permittivity of vacuum	(F/m)
ε	dielectric constant	(–)

REFERENCES

Borra, J.P., 2018, Review on water electro-sprays and applications of charged drops with focus on the corona-assisted cone-jet mode for high efficiency air filtration by wet electro-scrubbing of aerosols. Journal of Aerosol Science 125, 208-236.

Cho, Y., Kim, S., Lim, H., Choi, S., Kim, M., 2019, Experimental study of electrostatic spray modes of high-flowrate water with horizontal nozzle. Journal of Mechanical Science and Technology 33(9), 4563–4572.

Cloupeau, M., 1994, Recipes for use of EHD spraying in cone-jet mode and notes on corona discharge effects, Journal of Aerosol Science 25(6), 1143-1157.

Jaworek, A., Krupa, A., 1999, Classification of the Modes of EHD Spraying. Journal of Aerosol Science 30(7), 873-893.

Jung, M., Kim, S., Lim, J., Lee, J., Jeong, S., Ku, D., Na, I., Kim, M., 2022, Droplet Characterization of High-Flowrate Water Electrospray using Shadowgraph Image Analysis. Journal of Mechanical Science and Technology 36 (4) (2022), 2139~2148.

Kim, H.H., Kim, J.H., Ogata, A., 2011, Time-resolved high-speed camera observation of electrospray. Journal of Aerosol Science 42(4), 249-263.

Kim, S., Jung, M., Choi, S., Lee, J., Lim, J., Kim, M., 2020, Discharge current of water electrospray with electrical conductivity under high-voltage and high-flow-rate conditions. Experimental Thermal and Fluid Science 118, 110151.

Park, I., Kim, S.B., Hong, W.S., Kim, S.S., 2015, Classification of electrohydrodynamic spraying modes of water in air at atmospheric pressure. Journal of Aerosol Science 89, 26–30.

Tang, K., Gomez, A., 1994, On the structure of an electrostatic spray of monodisperse droplets. Physics of Fluids, 6(7), 2317–2332.

Taylor, G.I., 1966, The force exerted by an electric field on a long cylindrical conductor, Proceedings of the Royal Society A 291(1425), 145-158.

ACKNOWLEDGEMENT

This research was jointly supported by National Research Foundation of Korea (NRF No. 2019R1A2C108869414) and by Korea Institute of Energy Technology Evaluation and Planning (KETEP) (20202020900290, 20214000000280, 20212050100010) funded by Ministry of Trade, Industry and Energy. This research was also supported by the Korea Environmental Industry & Technology Institute (KEITI No. 2020003060005) Authors sincerely appreciate their supports.